Dalton Transactions

Accepted Manuscript

ROYAL SOCIETY OF CHEMISTRY

www.rsc.org/dalton

Journal Name

RSCPublishing

ARTICLE

Utilisation of water soluble iridium catalysts for Signal Amplification by Reversible Exchange

Cite this: DOI: 10.1039/x0xx00000x

M. Fekete,[a] C. Gibard,[b] G. J. Dear,[c] G. G. R. Green,[a] A. J. J. Hooper,[a] A. D. Roberts,[c] F. Cisnetti[b] and S. B. Duckett[a]

Received 00th January 2012,
Accepted 00th January 2012

DOI: 10.1039/x0xx00000x

www.rsc.org/

The catalytic hyperpolarisation of pyridine, 3-hydroxypyridine and oxazol by the Signal Amplification By Reversible Exchange (SABRE) process is achieved by a series of water soluble iridium phosphine and N-heterocyclic carbene dihydride complexes. While the efficiency of the SABRE process in methanol-d_4 solution or ethanol-d_6 solution is high, with over 400-fold ^{1}H polarisation of pyridine being produced by $[Ir(H)_2(NCMe)(py)(IMes)$(monosulfonated-triphenylphosphine)$]BF_4$, changing to a D_2O or a D_2O/ethanol solvent mixture leads to dramatically reduced activity which is rationalised in terms of low H_2 solubility.

Introduction

Ir^I-complexes containing both N-heterocyclic carbene (NHC) and phosphine ligands have been found to show very good catalytic activity in the homogeneous hydrogenation of olefins.[1] In the case of $[Ir(COD)(IMes)(P(^nBu)_3]PF_6$, where IMes is the N-heterocyclic carbene (NHC) 1,3-bis(2,4,6-trimethylphenyl)imidazol-2-ylidene, this activity has been studied by *Para*-Hydrogen Induced Polarization (PHIP) and hyperpolarised nuclear magnetic resonance (NMR) signals were seen in the ethyl proton resonances of the hydrogenation product ethylbenzene.[2] *Para*-hydrogen (p-H_2)[3] studies have been used to follow many such hydrogenation reactions and a number of reaction intermediates have been detected.[4-8]

Traditionally, two different effects are seen when reactions with p-H_2 are examined. These correspond to *Para*-hydrogen and Synthesis Allow Dramatically Enhanced Nuclear Alignment (PASADENA)[4, 5, 7] when the reaction proceeds in high magnetic field, and Adiabatic Longitudinal Transport After Dissociation Engenders Net Alignment (ALTADENA[9]) for reactions that occur in low magnetic field. Under both of these reaction conditions pairs of protons in the associated reaction products can be observed by NMR spectroscopy with enhanced intensity when they were previously located in the same molecule of p-H_2. Under PASADENA conditions these enhanced NMR signals appear with equal intensity and feature an anti-phase component that is separated by J_{HH}, the scalar coupling between the two p-H_2 derived protons. Under ALTADENA conditions, only one component of each proton signal is observed as an enhanced signal, although the two distinct resonances still differ in their relative phase (see ESI).

Recently, a range of iridium-complexes have been found to be active in an alternative p-H_2 based process that has become known as Signal Amplification By Reversible Exchange (SABRE).[10, 11] In this transformation, polarisation that was initially located on the two hydride ligands of a metal-dihydride complex moves into the proton nuclei of a weakly bound ligand in low field.[8, 6] Upon ligand dissociation, a hyperpolarised but chemically unmodified material can be produced. This process is catalytic in magnetisation transfer from p-H_2. The first reported studies used $[Ir(COD)(PCy_3)(py)]BF_4$[11] (py = pyridine) as the catalyst but greater hyperpolarisation efficiency proved to be delivered by the related catalyst precursor [Ir(COD)(IMes)Cl]. This observation was not surprising in as far as NHCs have found widespread use as replacements for phosphine ligands in inorganic chemistry[12, 13] and in many cases, this change leads to improved catalytic activity and complex stability.[14,2] A second generation of SABRE catalysts that are also based on iridium but now contain IMes and either PCy_3 or PPh_3 ligands have also been recently described.[15] The SABRE process has since been extended to operate with other NHCs[16, 17] and an array of substrates that includes nicotinamide, isoniazide,[18] pyrazinamide[19] and acetonitrile.[15]

The use of hyperpolarisation methods, such as those described here, is receiving significant attention because of the potential to collect *in vivo* data that may prove diagnostic of health.[20] The successful collection of *in vivo* data has already been demonstrated for a variety of hyperpolarisation routes which include PHIP but not yet SABRE.[21-24] In contrast, dynamic nuclear polarization (DNP) studies on pyruvate are already being undertaken in the clinic.[25-28] Consequently there is substantial interest in understanding the catalytic role of the metal in the SABRE process and in achieving the delivery of

biocompatible materials. We note that a number of studies have considered specific aspects of this process.[29,18,20]

One potential problem with completing such studies is the low solubility of H_2 in water. It has been quantified by several groups,[30-32] with the values of Linke[33] being widely used that are 14–15 times lower than those in ethanol. This suggests that H_2 may become a limiting reagent in water. H_2 is, however, slightly more soluble in ethanol than methanol.[34,35,36] We note that Münnemann *et al*. have reported one route to improve the flux of H_2 in aqueous solution.[37]

Here we report observations on a series of iridium(III) complexes that contain either water solubilizing phosphine or NHC ligands. Their synthesis, characterization and use in SABRE based polarisation transfer reactions are described. We use pyridine as the hyperpolarisation target in our model studies in order to allow us to compare the activity of the new complexes to that of previously reported $[Ir(H)_2(NCMe)_2(IMes)(PPh_3)]BF_4$ (**1a**) and $[Ir(H)_2(NCMe)(py)(IMes)(PPh_3)]BF_4$ (**2a**).[15] We then extend these studies to consider the related substrates oxazole and 3-hydroxypyridine which reflect more interesting hyperpolarisation targets (Scheme 1). By monitoring the SABRE effect in methanol, ethanol, ethanol-water mixtures, and water itself we seek to gain information on how to undertake SABRE catalysis in a biocompatible solvent medium such as that required for *in vivo* injection.

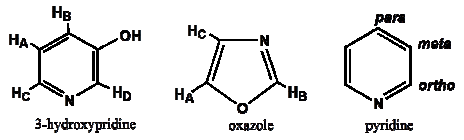

Scheme 1. Structure of 3-hydroxypyridine, oxazole and pyridine molecules.

We make use of the fact that sulfonation of PPh_3 at the *para* position, to form di-*para*-sulfonated triphenylphosphine (*p*tppds), and at the *meta* position to form mono-*meta*-sulfonated triphenylphosphine (mtppms) and *meta*-tri-sulfonated triphenylphosphine (*m*tppts) produces water soluble phosphine ligands.[38, 39] Complexes with such sulfonated-PPh_3 ligands have different activities to those of their parent, PPh_3, due to the change in steric and electronic properties that are associated with the functionalised phosphines. The solubility of these ligands is related to the ligand structure in aqueous solution where hydrophilic and hydrophobic moieties, possible self-association and micelle formation, play a role.[40 41 38 42] The sodium salt of *m*tppts is around 39 times more soluble in water than *m*tppms itself and we have therefore used sodium or potassium salts in this study.[43]

The position of the sulfonated group also influences the solubility, cone angle and activity of any complexes that are formed[40] and this may be relevant here when the activity of these systems towards SABRE is considered.[10,16, 17] The cone angle of the phosphine ligand increases with the number of sulfonated groups present in the *meta* position (PPh_3 146°, *m*tppms 152°, *m*tppts 160°).[43] However, when PPh_3 is sulfonated at the *para* position the product exhibits a similar cone angle to PPh_3 itself (PPh_3 146°, *p*tppms 138°, *p*tppts 139°).[44] Laurenczy and Dyson *et al.* found that the ruthenium catalysed generation of hydrogen from formic acid varied inefficiency as follows, *m*tppds > *m*tppts > *p*tppms > *m*tppms.[40]

The complexes we used here are based on the Ir^{III}-NHC-phosphine complex $[Ir(H)_2(IMes)(NCMe)_2(mtppts)]BF_4$ (**1b**) which has been reported by Torres *et al.*.[11, 39] The related complexes $[Ir(H)_2(NCMe)_2(IMes)(L)]BF_4$ (**1**) (L = *m*tppms (**1c**) and *p*tppds (**1d**)) were also employed (see ESI). We then extend these studies to include several water solubilised iridium complexes by functionalising their NHC ligands. The modification of the scaffold of an NHC ligand by adding a water-solubilizing groups (e.g. sulfonates, ammonium salts) is being actively investigated because of the importance of such ligands.[45,46] Related water-soluble Ir^{III}-NHC complexes have been used by Peris *et al.* for the reduction of CO_2 to formate[47, 48] and as well for the deuteration of aryl amines.[49]

Results and discussion

Water-soluble Iridium-IMes-phosphine complexes

Formation of $[Ir(H)_2(NCMe)(py)(IMes)(L)]BF_4$ (2). When the series of IMes complexes, **1**, react with a 20-fold excess of pyridine and dihydrogen in methanol-d_4 or D_2O the dominant products are the corresponding pyridine-acetonitrile adducts $[Ir(H)_2(NCMe)(py)(IMes)(L)]BF_4$ (**2**) (where L = PPh_3 (**2a**), *m*tppts (**2b**), *m*tppms (**2c**) and *p*tppds (**2d**), Scheme 2). These reactions were first monitored by ^1H NMR spectroscopy in a 5 mm NMR tube. In methanol-d_4 solution, the hydride signals of the PPh_3 analogue, **2a**, appear at δ –21.10 (J_{HH} = –7.2 Hz, J_{HP} = 18.4 Hz) and δ –22.30 (J_{HH} = –7.2 Hz, J_{HP} = 19.4 Hz), but they are not visible when the same reaction is undertaken in D_2O solution due to low solubility of **2a**. In contrast the *m*tppts

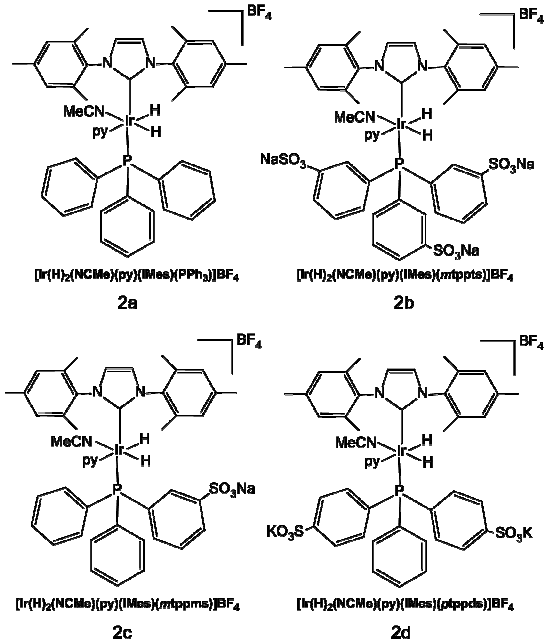

Scheme 2. Structure of complexes **2a-2b**.

derivative, **2b**, is soluble in both methanol-d_4 and D_2O solution.

In D_2O, the corresponding hydride ligand signals of **2b** appear at δ –21.07 (J_{HH} = –6.9 Hz, J_{HP} = 16.6 Hz) and δ –22.15 (J_{HH} = –6.9 Hz, J_{HP} = 18.4 Hz), while in methanol-d_4, they are visible at δ –21.07 (J_{HH} = –6.9 Hz, J_{HP} = 16.4 Hz) and δ –21.97 (J_{HH} = –6.9 Hz, J_{HP} = 18.1 Hz). For **2c**, the hydride signals appear at δ –21.05 and δ –22.17 in methanol-d_4, and at δ –21.08 and δ –22.08 in D_2O respectively. We note that the hydride chemical shifts for **2a**, **2b** and **2c** are therefore very similar, and that there is only a slight change in value with solvent. We also note that the pH of these solutions is ca. 7.

When a sample of **2c** is prepared using ^{15}N labelled pyridine, in methanol-d_4, the hydride signal at δ –22.17 (J_{HH} = 6.5 Hz, J_{HP} = 18.5 Hz) proved to exhibit an additional doublet splitting of 19.0 Hz due to the additional *trans* ^{15}N coupling. The higher field resonance observed in these complexes is therefore due to a hydride ligand which is *trans* to pyridine.[15] If the pyridine or CH_3CN ligands in these complexes were replaced by H_2O or methanol we would expect to see substantial differences in their chemical shift values with solvent.[50-52] We see no evidence for such species in these ^1H NMR spectra at 298 K which confirms that pyridine is a much better ligand than either methanol or water. The corresponding characterisation data for complexes **2**, and their precursors, is presented in the experimental.

The four low-field hydride chemical shifts exhibited by **2** for the ligand that is *trans* to NCMe lie within 20 Hz of each other. In contrast, those for the hydride sites that lie *trans* to pyridine differ by 132 Hz across the series. Such a change in chemical shift is consistent with L exhibiting a greater effect on the binding of pyridine when compared to acetonitrile.

Reactivity of 2 towards *para*-hydrogen. We then monitored the reactions of **1** and pyridine with *p*-H_2. The hydride signals of **2** all proved to show PHIP activity upon the application of a 45° *rf*. pulse as a consequence of their chemical inequivalence.[53] The result of this process is the observation of a pair of anti-phase hydride ligand signals, as exemplified in Fig. 1 for **2d**. The associated hydride ligand signals proved to have narrow line widths for all four ligand systems thereby suggesting that any exchange processes they exhibit are slow on the NMR timescale.

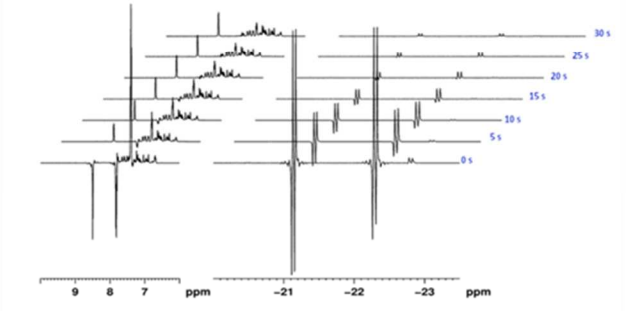

Figure 1. Series of ^1H NMR spectra collected on a methanol-d_4 sample of **2d** under *p*-H_2 showing how the strongly enhanced hydride resonances decay with reaction time. Pyridine signal amplification under SABRE is revealed in the t = 0 s measurement.

Upon examination of these NMR spectra, the order of the hydride ligand signal intensities, for comparable sample concentrations in methanol-d_4 under fresh *p*-H_2, proved to follow the trend **2c** > **2d** > **2b** > **2a**. These observations confirm that functionalization of the parent complex **1a** by sulfonation of the phosphine does not preclude PHIP activity but it does change their observed reactivity although all of these systems form **2** rapidly. The 45° *rf*. pulse we apply in these measurements probes the level of *p*-H_2 hyperpolarisation that is retained in the hydride ligands. We are therefore looking at a signal whose intensity reflects the purity of *p*-H_2 in solution, the level of retained hydride ligand polarisation, the hydride ligands relaxation time and the rate of *p*-H_2 exchange in **2**. Given the similarities that exist between these complexes, the first three of these four effects should be comparable, and hence it would seem sensible to suggest that the order of H_2 loss is **2c** > **2d** > **2b** > **2a**.

The associated hydride ligand signal intensities that were observed in a series of consecutive ^1H NMR spectra proved to decay over time as the *p*-H_2 present in solution is converted into normal H_2 (Fig. 1). The rate of decay of the observed hydride ligand signal intensities in these spectra proved to follow the trend **2c**~**2a** > **2b** > **2d** and does not therefore mirror the initial PHIP derived hydride ligand signal intensities (ESI).

The quenching of *p*-H_2 in these solutions is likely to be due to the formation of the dihydrogen-dihydride complex $[Ir(H)_2(H_2)(py)(IMes)(L)]BF_4$.[54, 55] This complex is analogous in nature to $[Ir(H)_2(H_2)(py)_2(IMes)]BF_4$ for which a similar role has been demonstrated in the exchange between free and bound H_2 which surprisingly has a rate that is proportional to the H_2 concentration even though this exchange process happens after dissociative pyridine loss.[11] The lifetime of this complex is critical, as the rapid relaxation that is associated with its dihydrogen ligand, when coupled with the chemical exchange flux, controls the rate of *p*-H_2 conversion into normal H_2. It would appear therefore that **2a** and **2c** access $[Ir(H)_2(H_2)(py)(IMes)(L)]BF_4$ most readily. We note, however, that the SABRE process itself will lead to a loss of polarisation in low-field and enhanced relaxation of the substrate in high field.[17]

Observation of signal amplification by reversible exchange. In addition to the PHIP that is seen in the hydride ligand resonances of these complexes, SABRE polarisation of the signals of free pyridine and acetonitrile is evident. This effect is seen in the corresponding single scan NMR measurements that are completed immediately after sample introduction (Fig. 1). This process is the result of the transfer of magnetisation from the hydride ligands of **2**, first into the bound pyridine and acetonitrile ligands, and then through ligand exchange into the free ligand pool in solution. This process occurs in low-field when the sample is shaken to equilibrate the *p*-H_2 in solution with that in the headspace above it. Furthermore, the observation of SABRE in the signals for free pyridine and acetonitrile serves to confirm that **2** undergoes ligand exchange. The optimal polarisation transfer field for the hyperpolarisation of the protons of acetonitrile proved to be 20

G in a series of related Ir^{III}-NHC-phosphine systems.[15] At this magnetic field, in methanol-d_4 with a 20 fold pyridine and 2 fold NCMe excess based on iridium, the total proton signal enhancement on NCMe seen for **2a** was 81 fold while the total pyridine proton signal enhancement was 62 fold. The acetonitrile enhancement level dropped for **2b** to a 5 fold (13 fold for pyridine) but for **2c** proved to be 36 fold (pyridine 107 fold) and for **2d** it was 21 fold (pyridine 39 fold). We note that using acetonitrile-d_3 instead of acetonitrile-h_3 did not change the level of polarisation transfer into pyridine.[15] It is therefore clear that these complexes show significantly different levels of SABRE activity.

Ligand exchange kinetics of 2. It has been previously reported that the lifetime of the polarisation transfer catalyst and the polarisation transfer field (PTF) are also important parameters in controlling the efficiency of this catalytic process.[8] The observed rate constants for acetonitrile and pyridine loss for **2** over the temperature range 290 K – 310 K are listed in Table S1. These values were determined by EXSY methods and H_2 elimination from **2c** was observed to proceed with an experimentally determined rate of 0.056 ± 0.002 s^{-1} at 300 K. For **2a** rapid HD exchange precluded the quantification the H_2 loss rate in methanol-d_4 solution and none was evident for the other two complexes. These observations are interesting given that the corresponding ^{1}H NMR measurements actually contain PHIP enhanced hydride ligand signals for all four complexes. Hence, while the EXSY method is too limited by relaxation to detect exchange on the NMR timescale by **2b** and **2d**, the use of *p*-H_2 reveals the existence of such a reaction pathway.

It has previously been reported that complex **2a** undergoes indirect pyridine exchange via an acetonitrile loss pathway.[15] This means that $[Ir(H)_2(NCMe)(py)(IMes)(L)]BF_4$ (**2**) acts first to form unstable $[Ir(H)_2(py)_2(L)(IMes)]BF_4$ by NCMe loss, and then this newly formed complex reacts further to reform **2** via pyridine loss. The quantified first order rate constants for the loss of acetonitrile at 300 K in **2a**, **2b**, **2c** and **2d** proved to be 0.966 ± 0.009 s^{-1}, 0.195 ± 0.003 s^{-1}, 0.559 ± 0.006 s^{-1} and 0.218 ± 0.001 s^{-1} respectively and mirror the SABRE acetonitrile enhancement trend described above. Furthermore, the observed pseudo rates of pyridine ligand loss at 300 K are indeed smaller, at 0.039 ± 0.004 s^{-1}, 0.0143 ± 0.0004 s^{-1}, 0.097 ± 0.001 s^{-1} and 0.040 ± 0.005 s^{-1} respectively, than those of acetonitrile loss. It is the arithmetic product of these two rates constants that therefore detail the comparative pyridine exchange flux, which proves to follow the observed trend in total pyridine signal enhancement (**2c** > **2a** > **2d** > **2b**). We note that these four effective pyridine loss rates are actually significantly smaller than the 23.4 s^{-1} value reported for the highly efficient SABRE catalyst $[Ir(IMes)(py)_3(H)_2]Cl$ referred to earlier.[11] They also fail to link with the ligands cone angle.

Polarisation transfer field effects on SABRE. Despite these slow rates of ligand exchange, we probed the efficiency of **2** for SABRE using an automated polariser that has been described elsewhere.[19, 56, 57] The order of SABRE pyridine polarisation efficiency in this equipment proved to be **2a** > **2c** > **2d** > **2b**, with **2a** delivering a 60-fold signal enhancement in the *meta* proton signal of free pyridine when the PTF was set to 10 G (see ESI) in methanol solution.

When the PTF was changed from 0.5–140 G, a significant variation in efficiency was seen, as shown in Fig. 2, where positive signal amplitudes proved to be present for all three free pyridine signals at all PTF values of less than 100 G. For comparison purposes the reported [Ir(COD)(IMes)Cl] derived system shows a 142-fold increase in signal strength for the *meta* proton of pyridine under these conditions when the PTF is 70 G, whilst the other two resonances show an emission signal of relative intensity 100 : 112 (*para* : *ortho*). This confirms that while **2** delivers a lower inherent polarisation transfer efficiency for pyridine than [Ir(COD)(IMes)Cl] its use benefits from the fact that the resulting signals now beneficially share a common phase. Furthermore, when **2c** is examined with a 19-fold pyridine excess and a 2.5 mM metal complex concentration, the total ^{1}H NMR signal enhancement level increases to 400 fold at 140 G. This compares to a 610 fold value with [Ir(COD)(IMes)Cl] at 70 G under similar reagent concentrations. The ability of **2c** to act as a SABRE catalyst in methanol is therefore impressive even though it exhibits slow ligand exchange.

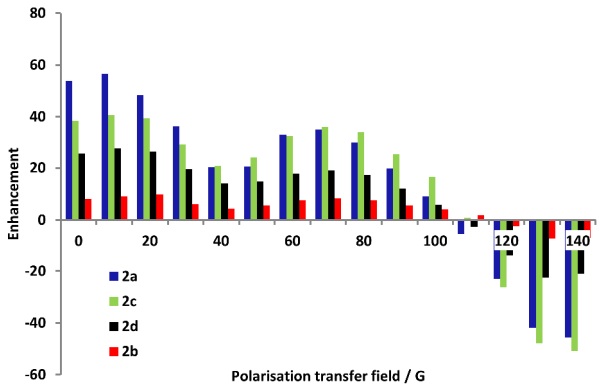

Figure 2. Polarisation transfer field dependence on the level of pyridine *meta* proton signal enhancement (fold) under SABRE at 298 K in methanol-d_4 solution when the concentration of **2** is 5.5 mM and a 19-fold excess of pyridine is present.

Achieving SABRE in a biocompatible solvent. We need, however, to consider the SABRE levels that can be achieved through catalysis in a biologically compatible solvent where **2** is still expected to be soluble. The first of these studies were undertaken in ethanol-d_6, the second in a 30% ethanol-water mixture and the third and final study in D_2O solution. The level of polarisation transfer with **2a** to pyridine molecules is 5 times lower in ethanol-d_6 than in methanol-d_4 (ESI, Fig. S5). Unfortunately the ^{1}H resonances of pyridine failed to show any SABRE in either the ethanol-water mixture or the D_2O solution. When we followed the required pyridine exchange process in D_2O for **2c** a rate of 0.06 ± 0.04 was estimated which is broadly comparable with the value in methanol. The corresponding H_2 loss could not, however, be followed.

This is because H/D exchange and deuteration of pyridine occurs very quickly in these D_2O containing solvent mixtures[49] with the result that there is a large error in the pyridine loss rate. In ethanol-d_6 solution, after just 2 hours, 30% of the protio form of the dihydride-complexes (**2**) are transformed into the corresponding HD-and D_2 isotopomers under 3 bar H_2 pressure. In D_2O solution, at 305 K after 62 hours all the protons of pyridine in the *meta* position are now deuterated with 40 % of the *ortho* and *para* sites also showing ^2H incorporation. These data confirm that complexes of this type are good catalysts for deuterium transfer.[58]

Extending SABRE to oxazole and 3-hydroxypyridine. We therefore examined the behaviour of the better performing SABRE catalyst precursor **1c** with the related substrates oxazole and 3-hydroxypyridine. The total proton signal enhancement of oxazole that is achieved with **1c** in methanol-d_4 solution proved to be 827 fold (Fig. S7), while in neat ethanol-d_6 the observed enhancement factor was 37% lower at 522-fold. These measurements were conducted under the same experimental conditions in order to make them comparable. Fig. S8 reveals this behaviour when a 5 fold excess of oxazole is used in conjunction with a 5.2 mM concentration of **1c** and a 60 G PTF. This observation would be consistent with slower oxazol loss given the higher H_2 solubility in ethanol when compared to methanol.[17]

Fig. 3 reveals that good SABRE activity results for 3-hydroxypyridine with **1c** in the ethanol-water mixture, although oxazole again failed to hyperpolarise in this solvent. Interestingly, 3-hydroxypyridine showed poorer SABRE activity in methanol-d_4, than oxazole, with the corresponding total proton polarisation transfer level at 70 G being just 71-fold (Fig. S10). In the case of the 30 % ethanol-water mixture the optimal magnetisation transfer field moved to 140 G and now a 62-fold total proton signal enhancement was observed. In methanol-d_4 the signals for proton C and D of 3-hydroxy-pyridine (see Scheme 1) overlap and possess absorption character over the PTF range 0-140 G, while in a 30 % ethanol-water mixture they possessed emission character above 110 G.

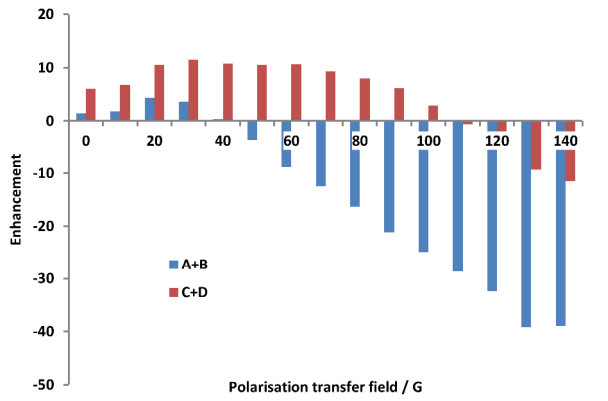

Figure 3. Polarisation transfer field dependence on the specified ^1H NMR signal intensities gains (fold) for 3-hydroxypyridine (see Scheme 1) achieved under SABRE at 307 K in a 30 % ethanol / 70 % D_2O mixture when the concentration of **2c** was 5.3 mM and a 3-fold excess of substrate was present.

Given these results, we decided that **2** is unlikely to meet the requirements of a high SABRE activity catalyst in a biocompatible medium, although its performance in ethanol-d_6 solution is acceptable. This would suggest therefore that the dilution of an ethanol solution after SABRE reflects the optimal way to produce a biocompatible sample for in vivo injection with **2**. As a consequence of this observation, we set out to prepare a series of complexes containing NHC ligands functionalised with solubilising groups that we hoped would be closer in behaviour to the highly active SABRE catalyst $[Ir(IMes)(py)_3(H)_2]Cl$.[17]

Water-soluble Ir-NHC-triazole catalysts

Synthesis of ligand precursors and complexes. We therefore prepared a series of water-soluble azolium salts as NHC ligands precursors (Scheme 3) wherein the common NHC motif is functionalised at the periphery by a triazole ring carrying a protic or a charged group. The functionalization step involved a copper-catalysed azide alkyne cycloaddition (CuAAC) reaction[59,60] This reaction was performed efficiently under Click conditions via a stable and active copper(I)-NHC complex[61,62] on synthetically accessible diamine[59] or diimine precursors (ESI).

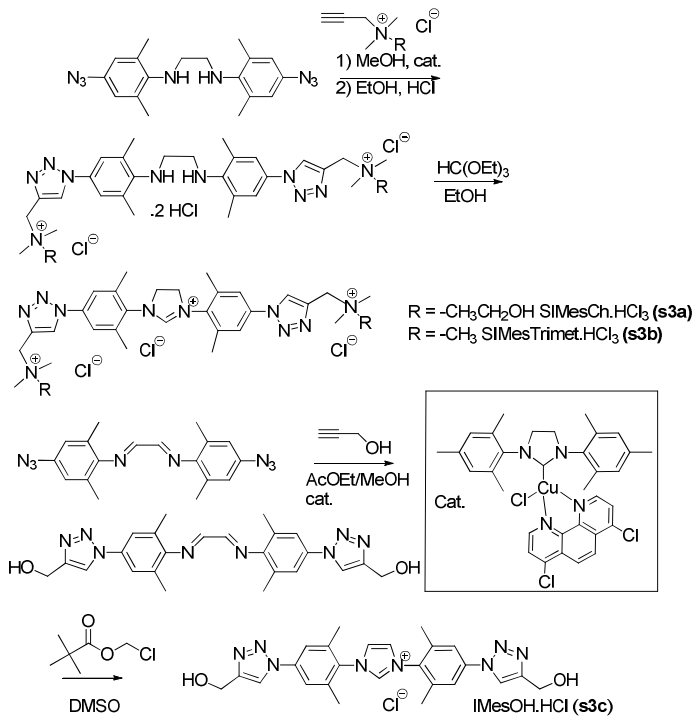

Scheme 3. Synthesis of azolium salts **s3a-s3c**. Insert: catalyst used for CuAAC cycloaddition reactions.

After introduction of the hydrophilic moieties, cyclisation was performed by reaction with pivaloyloxymethyl chloride

(POMCl, IMes-like backbone) as in our previous reports [60, 63] and for other hydrophilic compounds classically[64, 65] with triethyl orthoformate (SIMes-like backbone; SIMes: 1,3-Bis(2,4,6-trimethylphenyl)-imidazoline-2-ylidene). Preliminary experiments showed that CuAAC could also be performed on the diimine precursor with alkynes bearing ammonium salts. However, no efficient cyclisation conditions could be found in that case (attempted cyclisations with POMCl resulted in decomposition of the diimine group). In any case, changing from unsaturated IMes to saturated SIMes backbone is well-known to have a limited effect on the behaviour of the NHC ligand.[66]

Such prefunctionalised (for a discussion on pre- or post-functionalisation of metal-NHC complexes see a recent review [67]) azolium salts have been used previously by some of us to prepare hydrophilic metal–NHC complexes of Cu, Ag and Au that are analogous to the well-known IPr,[63, 67] SIPr[68] and SIMes[59] carbenes which find widespread use in organometallic chemistry. Here, the SIMes form bears a cationic quaternary ammonium groups that is derived from choline ($SIMesCh^{2+}$)[59] or trimethylammonium ($SIMesTrimet^{2+}$). Starting from these hydrophilic imidazol(in)ium salts, the necessary iridium(I)-NHC complexes (**3**) could be formed in basic conditions as shown in Scheme 4.

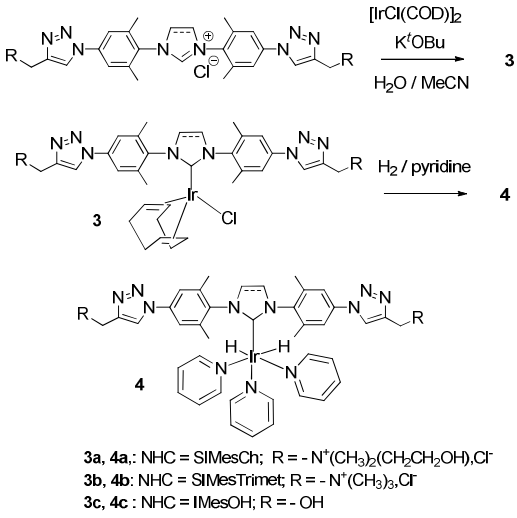

Scheme 4. Synthesis of iridium(I) NHC complexes and the formation of the corresponding Ir^{III} species upon reaction with H_2.

Polarisation transfer field effects on SABRE. Upon dissolving **3** in methanol-d_4 in the presence of pyridine and hydrogen a reaction takes place which sees the expected products $[Ir(H)_2(pyridine)_3(L)]^{x+}$ (**4**) form (L = SIMeCh, x = 3 (**4a**), SIMesTrimet, x = 3 (**4b**) and IMesOH, x = 1 (**4c**), see ESI). In the corresponding ^{1}H NMR spectra, a series of hydride resonances appear as singlets at δ –22.54, δ –22.72 and δ –22.66 respectively for these species. The pyridine ligand loss rate constant was determined for **4a** in methanol-d_4 solution at 300 K as 1.23 ± 0.08 s^{-1}, whilst that for **4b** proved to be 0.043 ± 0.003 s^{-1}. These two ligand loss rate constants are therefore smaller than that of $[Ir(IMes)(py)_3(H)_2]Cl$ and $[Ir(SIMes)(py)_3(H)_2]Cl$ (45.1 s^{-1}) [17] but comparable to those of **2**. **4a** exhibits the highest pyridine ligand exchange rate of either **2** or **4** at 300 K. In case of **4c** it was not possible to follow the ligand exchange process because it turned out to be very slow and there was evidence for fast ligand deuteration. A role for a dihydrogen-dihydride complex would also be expected in the formal H_2 loss mechanism.[11]

4 was then employed in a series of SABRE reactions with *p*-H_2 and pyridine in an analogous way to those described for **1**. Fig. 4 illustrates the PTF dependence on the pyridine ^{1}H polarisation level that is achieved by **4b** in methanol-d_4. Comparison with Fig. 2 reveals that different behaviour is evident.

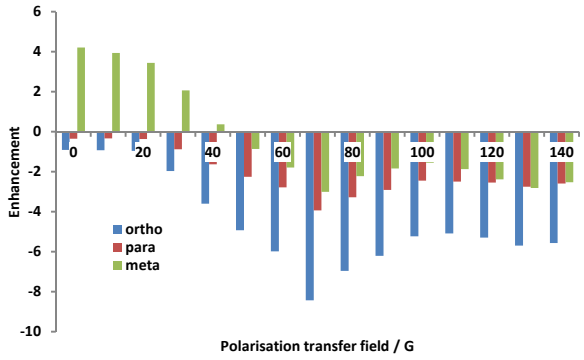

Figure 4. ^{1}H NMR signal enhancement (fold) profile for the specified protons of pyridine in methanol-d_4 solution under SABRE with **4b** as a function of PTF when a 19-fold pyridine excess is employed.

Now the most efficient magnetisation transfer catalysis is observed with a PTF of 70 G, and all three signals appear with negative amplitude for all PTF values between 50 and 140 G. The total pyridine proton signal enhancement value for **4b** is, however, just 30 at 70 G, whilst the corresponding value for **4c** is 10.

In contrast, the total pyridine proton signal enhancement achieved for **4a** at 60 G proved to be around 750 and was unaffected on changing from a 2-fold to 34-fold ligand excess (767 vs 748, Fig. S2). This pyridine signal enhancement factor is superior that achieved by **2**, **4b** and **4c** and is consistent with the higher pyridine ligand exchange rate which enables transfer into a large number of molecules per unit time. We can therefore deduce that **4a** is the best SABRE catalyst of this series.

These complexes were then examined in a 67% D_2O, 3% dmso, 30% EtOH mixture. We added dmso to this mixture in order to improve hydrogen solubility and note that polarization transfer into dmso was not observed. While **4a** and **4b** proved to readily form in this solvent system, the total signal enhancement seen for the protons of pyridine that result from SABRE catalysis was just 9.4- and 3–fold respectively when the PTF was 0 G. No SABRE activity for **4c** is observed. The resulting PTF variation observed with **4a** in this biocompatible medium is shown in Fig. 5. We can therefore conclude that

these catalysts also exhibit poor solvent tolerance. We note that when **2** was examined with the dmso containing solvent mixture, magnetisation transfer ceased, even though no new complexes were detected. Given that dmso can act as a ligand it is likely that its coordination accounts for this change.[69]

Changing the substrate from pyridine to 3-hydroxypyridine and employing the biocompatible solvent mixture (30% ethanol and 70% D_2O) resulted in the observation of a 22-fold ^1H signal enhancement under SABRE at an 80 G PTF with **4a**. In methanol-d_4 solution, under the same experimental conditions, the total proton signal enhancement observed in the pool of free 3-hydroxypyridine proved to be almost double this value at 50-fold (Fig. S11)). Polarisation could also be transferred into oxazole in methanol-d_4 solution with the corresponding total proton signal enhancement being 23.7 (Fig. S9) at 60 G, and 2.7 in the ethanol mixture. Fig. 6 shows how the total proton signal enhancement varies for the specified substrates in mixture of 70% D_2O and 30% EtOH with **4a**. The signal enhancement for 3-hydroxypyridine in this solvent mixture is therefore far stronger than that of either oxazole or pyridine but still very low compared to that achieved in pure methanol or ethanol.

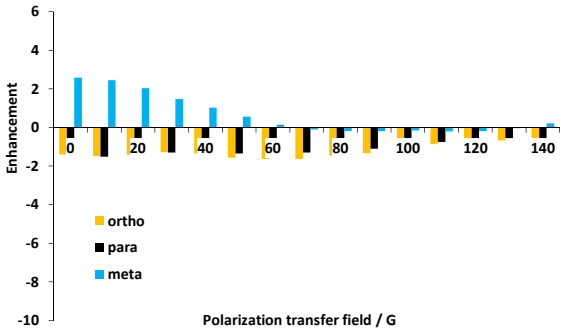

Figure 5. ^1H NMR signal enhancement (fold) profile as a function of PTF for the specified proton resonances of pyridine under SABRE in mixture of 67 % D_2O, 3 % dmso and 30 % EtOD with **4a** and a 19-fold pyridine excess.

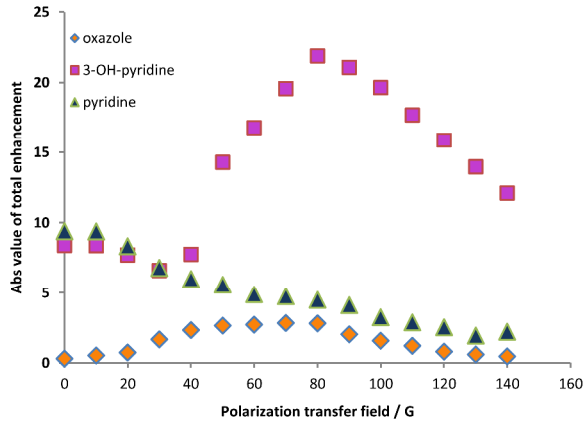

Figure 6. Total ^1H NMR signal enhancements (fold) observed for the specified substrate in a 70 % D_2O / 30 % EtOD mixture under SABRE with **4a** as a function of PTF. The concentration of **4a** was 5.3 mM, a 5 fold substrate excess and a temperature of 307 K was employed.

In one final test, we added 2 equivalents of NCMe to these solutions. The result of this process is the formation of the corresponding acetonitrile adducts $[Ir(H)_2(pyridine)(NCMe)(L)]^{x+}$ (**5**) (L = SIMeCh, x = 3 (**5a**), SIMesTrimet, x = 3 (**5b**) and IMesOH, x = 1 (**5c**), see ESI for their hydride signals NMR shifts). The efficiency of these complexes as polarisation transfer catalysts in methanol-d_4 proved to be comparable to those of **4** (Fig. S12, ESI). We also added one equivalence of PPh_3 to these solutions to test whether complexes of the type $[Ir(H)_2(pyridine)_2(PPh_3)(L)]^{x+}$ might function as SABRE catalysts but found no evidence for activity.[14]

Conclusions

In this paper we have prepared a series of water soluble phosphine and carbene complexes that are able to catalyse the SABRE effect. The phosphine complexes that were involved in this process are $[Ir(H)_2(NCMe)(py)(IMes)(L)]BF_4$ (**2**) (where L = PPh_3 (**2a**), *m*tppts (**2b**), *m*tppms (**2c**), *p*tppds (**2d**)). These complexes proved to function well in methanol solution for the SABRE of pyridine but showed lower activity than that previously reported for $[Ir(IMes)(py)_3(H)_2]Cl$. These complexes proved to be readily soluble in aqueous solvent medium. However, in this solvent mixture, or D_2O, they failed to catalyse the SABRE of pyridine under these conditions where there is low H_2 solubility and therefore a reduced rate of magnetisation transfer. They do, however, catalyse the ^2H labelling of pyridine in these solvents.

Given the improvements in activity that have been reported previously when the phosphine ligand in a SABRE catalyst is replaced by an NHC, three further complexes were prepared. These complexes led to the formation of $[Ir(H)_2(pyridine)_3(L)]^{x+}$ (**4**) (L = SIMesCh, x = 3 (**4a**), SIMesTrimet, x = 3 (**4b**) and IMesOH, x = 1 (**4c**)) as the active SABRE catalyst. They proved to function well in methanol and ethanol solution with **4a** proving to be the most active catalyst studied here. However, upon changing to a biocompatible solvent mixture or D_2O their activity was again dramatically reduced. This lower activity can be explained by the lower H_2 solubility in water.

As a consequence of this reduction in SABRE activity we also tested the substrates oxazole and 3-hydroxypyridine. Both of these materials proved to polarise well in methanol solution, but poor SABRE activity was again evident in the water mixtures, although improved activity was seen in them when compared to pyridine. On the basis of these tests, we conclude that polarisation transfer in ethanol and subsequent dilution reflects the best route to produce a biocompatible sample with these catalysts. It is also clear, however, that while SABRE catalysis is affected by the substrate these differences are less significant than the solvent effect.

Experimental

Materials and methods

All experimental procedures involving the iridium complexes were carried out under dinitrogen using standard

Schlenk techniques or an MBraun Unilab glovebox. General solvents for synthetic chemistry were dried using an Innovative Technology anhydrous solvent system or distilled from an appropriate drying agent under N_2 as necessary. Synthesis of hydrophilic azolium salts was performed without any precautions, unless noted. Deuterated solvents (methanol-d_4, benzene-d_6, $CDCl_3$, acetonitrile-d_3, dmso-d_6, D_2O) were obtained from Sigma-Aldrich and used as supplied. Tricyclohexylphosphine (PCy_3), triphenylphosphine (PPh_3) and bis(p-sulfonatophenyl)phenylphosphine dihydrate potassium salt (*p*tppbs) were obtain from Sigma-Aldrich. Diphenyl(m-sulfonatophenyl)phosphine dihydrate sodium salt (*m*tppms) and tris(3-sulfonatophenyl)phosphine hydrate sodium salt (*m*tppts) were obtained from Strem Chemicals, Inc.

The synthesis of $[Ir(H)_2(NCMe)_2(IMes)(mtppts)]BF_4$ (**1b**) has be described by Torres *et al.*[30] SIMeCh.HCl_3 and *N*,*N*′-bis(4-azido-2,6-dimethylphenyl)-ethane-1,2-diamine were prepared according to Gaulier *et al.*[59]

Synthesis and characterisation $[Ir(H)_2(NCCH_3)_2(IMes)(mtppms)]BF_4$ (1c): 0.243 g (0.35 mmol) of **1** was dissolved in 60 mL dry acetone and 0.14 g (0.35 mmol) *m*tppms added to form a magenta solution. 0.15 mL of dry acetonitrile (8 eq) and 1 atm of H_2 were then added over 4 hours. Slowly a bright yellow solution formed. The solvent is removed by vacuum and the product washed with cold diethyl ether (2 x 5 mL). Yield 0.243 g (70%) of a beige powder. ^{1}H NMR (400 MHz, C_6D_6, 298 K): δ -21.71 (d, 2H, J_{HP} = 17.4 Hz), 1.39 (s, 6H, $NCCH_3$), 1.88 (s, 12H, 4x -CH_3 of IMes), 2.11 (s, 6H, -CH_3), 6.08 (s, 4H, -CH=), 6.95 - 7.34 (m, 14H, –CH=, *m*tppms), 7.05, 7.11 (both s, NCH=CHN). $^{31}P\{^1H\}$ NMR (162 MHz, C_6D_6, 298 K): δ 18.06 ppm. ^{11}B NMR (160 MHz, C_6D_6, 298 K): -1.34 ppm. ^{19}F NMR (470 MHz, C_6D_6, 298 K): δ -153.92 (s, $^{10}BF_4$, 19%) and -153.97 (s,$^{11}BF_4$, 81%). $^{13}C\{^1H\}$ NMR (101 MHz, C_6D_6, 298 K): δ 1.5 ($NCCH_3$), 17.2, 20.2 (–CH_3), 118.2 (NCMe), 122.5, 127.2 (-N-CH=), 127.9 (d, J_{CP} = 10.1Hz), 128.5, 129.8 (s, -CH=, *m*tppms), 129.9, 130.3 (d, -CH=, J_{CP} = 13.8 Hz), 132.3 (d, -CH=, J_{CP} = 26.8 Hz), 132.5 (d, -CH=, J_{CP} = 8.2 Hz), 132.9, 133.9 (d, -CH=, J_{CP} = 11.5 Hz) 135.7, 137.4, 138.6 (s, –C=, IMes), 147.3 (d, -C_{SO3Na}, J_{CP} = 9.6 Hz) , 163.6 (d, –NCN=, J_{CP} = 114.5 Hz) ppm . ESI MS: 904.23 [M^+-NCMe], 861.19 [M^+-(2NCMe and 2H-)], 839.20 [M^+-(2NCMe, Na^+ and H^-)]

$[Ir(H)_2(NCCH_3)_2(IMes)(ptppds)]BF_4$ (1d): 0.115 g (0.215 mmol) of bis(*p*-sulfonatophenyl)phenylphosphine dihydrate dipotassium was dissolved in 0.5 mL degassed water at pH 10. This solution was added to 0.15 g (0.215 mmol) of $[Ir(IMes)(COD)(CO(CH_3)_2)]BF_4$ in 3.6 mL of degassed acetonitrile. The solution initially has a red colour. 1 atm H_2 was bubbled through the solution over 4 hours. Slowly a bright yellow solution is formed. The solvent is removed by vacuum and the product was with cold pentane (2 x 5 mL). Yield 0.21 g (85 %) of a beige powder. ^{1}H NMR (400 MHz, 298K, acetonitrile-d_3): δ -21.61 (d, 2H, J_{HP} = 17.31 Hz), 1.52 (s, 6H, $NCCH_3$), 2.08 (s, 12H, 4x -CH_3 of IMes), 2.34 (s, 6H, -CH_3), 6.89 – 7.51 (m, 19H, –CH=, *p*tppbs) ppm. $^{13}C\{^1H\}$ NMR (101 MHz, 298K, acetonitrile-d_3): δ 0.48 ($NCCH_3$), 17.24, 20.27, 26.34 (–CH_3), 118.20 (NCMe), 122.3 (-N-CH=), 124.69 (d, -CH=, J_{CP}=11.7 Hz), 125.17 (d, -CH=, J_{CP} = 7.24 Hz), 127.97 (-N-CH=), 128.37 (m, -CH=), 128.78 (d, -CH=, J_{CP} = 10.9 Hz), 130.05, 131.98, 132.51 (all three s, -CH=), 132.89 (d, -CH=, J_{CP} = 10.02 Hz), 133.45 (d, -CH=, J_{CP} = 15.04 Hz), 134.00 (d, -CH=, J_{CP} = 10.58 Hz), 134.56, 135.04, 135.94, 137.54, 139.1 (–C=), 146.57 (d, -C_{SO3K}, J_{CP} = 2.34 Hz) , 162.44 (d, –NCN=, J_{CP} = 114.7 Hz) ppm .$^{31}P\{^1H\}$ NMR (162 MHz, 298K, acetonitrile-d_3): 19.08 ppm. ^{11}B NMR (160 MHz, acetonitrile-d_3, 298K): -1.40 (s, $^{11}BF_4$, 81%) and -1.42 (s, $^{10}BF_4$, 19%) ppm. ^{19}F NMR (470 MHz, acetonitrile-d_3, 298 K): δ -152.89 (s, $^{10}BF_4$, 19%) and -152.94 (s, $^{11}BF_4$, 81%). ESI MS: 919.16 [M^+- (2 NCMe and 2 K^+)].

The synthesis for the ligands required for **3** can be found in the ESI.

[Ir(SIMesCh)(COD)Cl] (3a): Procedure 1: 0.22 g (0.304 mmol) of SIMeCh.HCl_3 (**s3a**), 0.03 g (0.555 mmol) sodium methoxide and 0.1 g (0.149 mmol) $[IrCl(COD)]_2$ were dissolved in a mixture of 10 mL dmso and 10 mL ethanol. The solution was stirred for 16.5 hours at room temperature. The solvents were removed slowly using a rotary evaporator at 50°C. The yield was 0.185 g (65 %). ^{1}H NMR (400 MHz, dmso-d_6, 298 K): δ 1.60 – 1.97 (m,-CH_2-, COD), 2.57-2.53 (br, 12H, -CH_3, arom), 3.15 (m, 12H, N^+-CH_3), 4.62 (s, 4H, -CH=, COD), 4.87(d, J_{HH} = 5.95 Hz), 5.49 (br, 2H, OH), 7.77 (s, 2H, HAr), 7.83 (s, 2H, HAr), 9.13 (s, 1H, $H_{triazole}$), 9.19 (s, 1H, $H_{triazole}$). $^{13}C\{^1H\}$ NMR (101 MHz, dmso-d_6, 298 K): δ 20.1, 22.8 (CH_3, arom,), 28.6 (-CH_2-, COD), 30.1 (arom, CH_3), 33.5 (-CH_2-, COD), 50.9 ($N(CH_3)_2$), 51.0 (-CH=, COD), 55.6 (CH_2OH), 83.5 (-CH=, COD), 119.7, 120.5 (-CH=, arom), 120.9 (-CH=, triazole), 133.9, 135.8, 136.8, 137.0, 137.3, 138.6, (-C=, $C_{aromatic}$), 139.7 (2 –$C(CH_3)$-), 139.6 (NCHN, $C_{triazol}$), 161.2 (Ir-C)).

Procedure 2: 0.130 g (0.194 mmol) of $[IrCl(COD)]_2$ was dissolved in 5 mL NCMe. 0.2390 g (0.389 mmol) of the SIMesCh.HCl ligand dissolved in 10 mL degassed H_2O. The aqueous solution of the ligand was added into the NCMe solution of the iridium dimer. 0.043 g (0.389 mmol) of KO^{t}Bu is added to the solution. When all the KO^{t}Bu was dissolved, 10 mL more NCMe was added and stirred at room temperature for 4 hours. The solvent was removed by vacuum. The Schlenk tube with the sticky product was cooled in liquid N_2 and was treated with diethyl ether to afford orange-brown solid. The solid was separated by decantation, washed with diethyl ether, and dried in vacuo. Yield was: 0.172 g (70 %). ^{1}H NMR (500 MHz, D_2O, 298 K): δ 1.60 – 2.25 (m,-CH_2-, COD), 2.50 (s, 12H, arom, -CH_3), 3.18 (12H, $(CH_3)_2$-N^+), 3.53 (s, 4H, -CH_2-N^+), 4.12 (4H, CH_2-OH), 4.61 (4H, -CH_2-imid), 4.77 (s, 4H, -CH=, COD), 4.82 (s, 4H, -CH_2-$C_{triazol}$), 7.71 (s, 4H, -CH=, HAr,), 8.81 (s, 2H, -CH=, $H_{triazole}$). $^{13}C\{^1H\}$ NMR (101 MHz, D_2O, 298 K): δ 17.0 , 21.1 (CH_3, arom,) 30.0 (-CH_2-, COD), 50.7 (-CH_2-, imid), 52.9 ($N^+(CH_3)_2$), 58.9, 64.1, (-CH_2-, around triazol), 120.8 (-CH=, COD), 127.3 (-CH=, triazol), 130.4 (-CH=, COD), 133.4, 136.1, 138.4, (-C=, arom, triazol), 176.9 (Ir-C).

[Ir(SIMesTrimet)(COD)Cl] (3b): 0.130 g (0.194 mmol) of $[IrCl(COD)]_2$ was dissolved in 5 mL NCMe. 0.234 g (0.39

mmol) of SIMesTrimet.HCl ligand dissolved in 10 mL degassed H_2O and 0.044 g (0.4 mmol) of KO^{t}Bu was added to the solution. The aqueous solution of the ligand was added into the NCMe solution of the iridium dimer and a further 10 mL of NCMe added. The solution was then stirred at room temperature for 6 hours, after which point, the solvent was removed under vacuum. The schlenk tube with the sticky red-orange product was then cooled and treated with diethyl ether to afford orange-brown solid. The solid was separated by decantation, washed with diethyl ether, and dried in vacuo. Yield was: 0.255g (70 %). ^{1}H NMR (500 MHz, D_2O, 298 K): δ 1.78 – 2.25 (m, 8H, -CH_2-, COD), 2.49 (s, 12H, arom,-CH_3), 3.16 (18H, $(CH_3)_3$-N^+), 4.60 (4H, -CH_2-imid), 4.72 (s, 4H, -CH=, COD), 4.74 (s, 4H, N^+-CH_2-Ctriazol), 7.71 (s, 2H, -CH=, HAr,), 8.80 (s, 2H, -CH=, Htriazole). ^{13}C{^{1}H} NMR (101 MHz, D_2O, 298 K): δ 17.2, 21.0, (CH_3, arom)) 31.3 (-CH_2-, COD), 50.9 (-CH_2-imid), 52.9 ($N^+(CH_3)_3$), 59.7 (-CH_2-, COD), 83.8, (-CH=, COD), 121.2 (-CH=, arom), 127.3 (-CH=, triazol), 133.8, 135.3, 135.9, 136.7, 138.3 (-C=, arom, triazol), 185.9 (Ir-C). ^{15}N{^{1}H} NMR (40.5 MHz, D_2O, 298 K): δ 49.7 ($N^+(CH_3)_2$), 133.4 (N_{imidaz}), 255.9 and 258.9 ($N_{triazol}$).

[Ir(IMesOH)(COD)Cl] (**3c**): 0.144 g (0.215 mmol) of $[IrCl(COD)]_2$ was dissolved in 10 mL NCMe. 0.230 g (0.43 mmol) of IMesOH.HCl and 0.049 g (0.44 mmol) of KO^{t}Bu were dissolved in mixture of 5 mL degassed H_2O and 10 mL NCMe under N_2. The aqueous solution was added into the NCMe solution of the iridium dimer, and stirred at room temperature for 4 hours. The solvent was removed by vacuum and a beige-brown powder remained as the product. Yield was: 0.277 g (85%). ^{1}H NMR (500 MHz, D_2O, 298 K): δ 1.78 – 2.25 (m,-CH_2-, COD), 2.84 (4H, -CH_2-imid), 2.31 (s, 12H, $CH(CH_3)_2$), 4.49 (s, 4H, -CH=, COD), 4.85 (s, 4H, -CH_2-Ctriazol), 7.80 (s, 2H, -CH=, HAr), 8.04 (s, 2H, -CH=, Htriazole), 8.49 (s, 2H, -CH=, Himid). ^{13}C{^{1}H} NMR (101 MHz, D_2O, 298 K): δ 16.9(CH_3, arom), 24.9 (-CH_2-, COD), 50.9 (-CH_2-imid), 57.0 (-CH_2-Ctriazol), 79.7 (-CH=, COD), 121.1 (-CH=, arom), 122.4 (-CH=, imid), 124.9 (-CH=, triazol), 133.4, 137.5, 138.3 (-C=, arom), 147.5 (-C=, imid) 173.6 (Ir-C).

Acknowledgements

The authors thank Bruker Biospin UK for a *para*hydrogen polarizer. The EPSRC (EP/G009546/1), the Wellcome Trust (092506 and 098335), the University of York and Oxford Instruments are also thanked. C. Gibard and F. Cisnetti acknowledge the Auvergne Region (France) for funding (PNC). Aurélie Rago and Ludivine Larue participated to this study as an undergraduate project. We are also grateful the GlaxoSmithKlein and the EPSRC (studentship A. J. J. Hooper).

Notes and references

[a]Centre for Hyperpolarization in Magnetic Resonance, University of York, York Science Park, York, YO10 5NY, UK.

[b]Institut de Chimie de Clermont-Ferrand Clermont Université, Université Blaise Pascal and CNRS, BP 10448, F-63000 Clermont-Ferrand, France.

[c]GlaxoSmithKline Research & Development Limited, Park Road, Ware, Hertfordshire, SG12 0DP, UK.

Electronic Supplementary Information (ESI) available: sample preparation, signal enhancements and raw data. See DOI: 10.1039/b000000x/

1. H. M. Lee, T. Jiang, E. D. Stevens and S. P. Nolan, *Organomet.*, 2001, **20**, 1255-1258.
2. L. D. Vazquez-Serrano, B. T. Owens and J. M. Buriak, *Chem. Commun. (Cambridge, U. K.)*, 2002, 2518-2519.
3. K. F. Bonhoeffer and P. Harteck, *Z. Elektrochem. Angew. Phys. Chem.*, 1929, **35**, 621-623.
4. C. R. Bowers and D. P. Weitekamp, *Phys. Rev. Lett.*, 1986, **57**, 2645-2648.
5. C. R. Bowers and D. P. Weitekamp, *J. Am. Chem. Soc.*, 1987, **109**, 5541-5542.
6. P. D. Morran, S. A. Colebrooke, S. B. Duckett, J. A. B. Lohman and R. Eisenberg, *J. Chem. Soc., Dalton Trans.*, 1998, 3363-3366.
7. T. C. Eisenschmid, R. U. Kirss, P. P. Deutsch, S. I. Hommeltoft, R. Eisenberg, J. Bargon, R. G. Lawler and A. L. Balch, *J. Am. Chem. Soc.*, 1987, **109**, 8089-8091.
8. R. A. Green, R. W. Adams, S. B. Duckett, R. E. Mewis, D. C. Williamson and G. G. R. Green, *Prog. Nucl. Magn. Reson. Spectrosc.*, 2012, **67**, 1-48.
9. M. G. Pravica and D. P. Weitekamp, *Chem. Phys. Lett.*, 1988, **145**, 255-258.
10. K. D. Atkinson, M. J. Cowley, P. I. P. Elliott, S. B. Duckett, G. G. R. Green, J. López-Serrano and A. C. Whitwood, *J. Am. Chem. Soc.*, 2009, **131**, 13362-13368.
11. M. J. Cowley, R. W. Adams, K. D. Atkinson, M. C. R. Cockett, S. B. Duckett, G. G. R. Green, J. A. B. Lohman, R. Kerssebaum, D. Kilgour and R. E. Mewis, *J. Am. Chem. Soc.*, 2011, **133**, 6134-6137.
12. J. Huang, L. Jafarpour, A. C. Hillier, E. D. Stevens and S. P. Nolan, *Organomet.*, 2001, **20**, 2878-2882.
13. J. Huang, E. D. Stevens, S. P. Nolan and J. L. Petersen, *J. Am. Chem. Soc.*, 1999, **121**, 2674-2678.
14. W. A. Herrmann, *Angew. Chem., Int. Ed.*, 2002, **41**, 1290-1309.
15. M. Fekete, O. Bayfield, S. B. Duckett, S. Hart, R. E. Mewis, N. Pridmore, P. J. Rayner and A. Whitwood, *Inorg. Chem.*, 2013, **52**, 13453-13461.
16. B. J. A. van Weerdenburg, S. Gloggler, N. Eshuis, A. H. J. Engwerda, J. M. M. Smits, R. de Gelder, S. Appelt, S. S. Wymenga, M. Tessari, M. C. Feiters, B. Blumich and F. P. J. T. Rutjes, *Chem. Commun. (Cambridge, U. K.)*, 2013, **49**, 7388-7390.
17. L. S. Lloyd, A. Asghar, M. J. Burns, A. Charlton, S. Coombes, M. J. Cowley, G. J. Dear, S. B. Duckett, G. R. Genov, G. G. R. Green, L. A. R. Highton, A. J. J. Hooper, M. Khan, I. G. Khazal, R. J. Lewis, R. E. Mewis, A. D. Roberts and A. J. Ruddlesden, *Cat. Sci. Tech.*, 2014, **4**, 3544-3554.
18. H. Zeng, J. Xu, J. Gillen, M. T. McMahon, D. Artemov, J.-M. Tyburn, J. A. B. Lohman, R. E. Mewis, K. D. Atkinson, G. G. R. Green, S. B. Duckett and P. C. M. van Zijl, *J. Magn. Reson.*, 2013, **237**, 73-78.
19. E. B. Dücker, L. T. Kuhn, K. Münnemann and C. Griesinger, *J. Magn. Reson.*, 2012, **214**, 159-165.

20. J.-B. Hövener, N. Schwaderlapp, R. Borowiak, T. Lickert, S. B. Duckett, R. E. Mewis, R. W. Adams, M. J. Burns, L. A. R. Highton, G. G. R. Green, A. Olaru, J. Hennig and D. von Elverfeldt, *Anal. Chem.*, 2014, **86**, 1767-1774.
21. P. Bhattacharya, E. Y. Chekmenev, W. F. Reynolds, S. Wagner, N. Zacharias, H. R. Chan, R. Bünger and B. D. Ross, *NMR in Biomedicine*, 2011, **24**, 1023-1028.
22. P. Lee, W. Leong, T. Tan, M. Lim, W. Han and G. K. Radda, *Hepatology*, 2013, **57**, 515-524.
23. M. D. Lingwood, T. A. Siaw, N. Sailasuta, O. A. Abulseoud, H. R. Chan, B. D. Ross, P. Bhattacharya and S. Han, *Radiology*, 2012, **265**, 418-425.
24. M. Mishkovsky, T. Cheng, A. Comment and R. Gruetter, *Mag. Res. Med.*, 2012, **68**, 349-352.
25. J. H. Ardenkjær-Larsen, B. Fridlund, A. Gram, G. Hansson, L. Hansson, M. H. Lerche, R. Servin, M. Thaning and K. Golman, *Proc. Natl. Acad. Sci. U. S. A.*, 2003, **100**, 10158-10163.
26. A. B. Barnes, G. De Paëpe, P. C. A. van der Wel, K. N. Hu, C. G. Joo, V. S. Bajaj, M. L. Mak-Jurkauskas, J. R. Sirigiri, J. Herzfeld, R. J. Temkin and R. G. Griffin, *Appl. Magn. Reson.*, 2008, **34**, 237-263.
27. K. H. Sze, Q. Wu, H. S. Tse and G. Zhu, *Top. Curr. Chem.*, 2012, **326**, 215-242.
28. D. M. Tesch and A. A. Nevzorov, *J. Magn. Reson.*, 2014, **239**, 9-15.
29. M. L. Truong, F. Shi, P. He, B. Yuan, K. N. Plunkett, A. M. Coffey, R. V. Shchepin, D. A. Barskiy, K. V. Kovtunov, I. V. Koptyug, K. W. Waddell, B. M. Goodson and E. Y. Chekmenev, *J. Phys. Chem. B*, 2014, **118**, 13882-13889.
30. L. Braun, *J. Phys. Chem.*, 1900, **5**, 79-80.
31. T. E. Crozier and S. Yamamoto, *J. Chem. Eng. Data*, 1974, **19**, 242-244.
32. T. J. Morrison and F. Billett, *J. Chem. Soc. (Resumed)*, 1952, 3819-3822.
33. Purwanto, R. M. Deshpande, R. V. Chaudhari and H. Delmas, *J. Chem. Eng. Data*, 1996, **41**, 1414-1417.
34. M. Safamirzaei, H. Modarress and M. Mohsen-Nia, *Fluid Phase Equilibria*, 2010, **289**, 32-39.
35. M. S. Wainwright, T. Ahn, D. L. Trimm and N. W. Cant, *J. Chem. Eng. Data*, 1987, **32**, 22-24.
36. R. B. Pirketta Scharlin, Estanislao Silla, Inaki Tunon and Juan Luis Pascual-Ahui, *Pure Appl. Chem.*, 1998, **70**, 1895-1904.
37. M. Roth, P. Kindervater, H.-P. Raich, J. Bargon, H. W. Spiess and K. Münnemann, *Angew. Chem., Int. Ed.*, 2010, **49**, 8358-8362.
38. F. J. I. T. Horváth, *Aqueous Organometallic Chemistry and Catalysis*, Kluwer Academic Publishers, Dordrecht, The Netherlands, 1995.
39. O. Torres, M. Martín and E. Sola, *Organomet.*, 2009, **28**, 863-870.
40. W. Gan, C. Fellay, P. J. Dyson and G. Laurenczy, *J. Coord. Chem.*, 2010, **63**, 2685-2694.
41. F. Joó, É. Papp and Á. Kathó, *Topics in Catalysis*, 1998, **5**, 113-124.
42. J. B. Graham Wright, *Acta Chem. Scand.*, 1962, **16**, 1262-1270.
43. M. R. Barton, Y. Zhang and J. D. Atwood, *J. Coord. Chem.*, 2002, **55**, 969-983.
44. G. Papp, J. Kovács, A. C. Bényei, G. Laurenczy, L. Nádasdi and F. Joó, *Can. J. Chem.*, 2001, **79**, 635-641.
45. K. H. Shaughnessy, *Chem. Rev. (Washington, DC, U. S.)*, 2009, **109**, 643-710.
46. L.-A. Schaper, S. J. Hock, W. A. Herrmann and F. E. Kühn, *Angew. Chem., Int. Ed.*, 2013, **52**, 270-289.
47. S. Sanz, A. Azua and E. Peris, *Dalton Trans.*, 2010, **39**, 6339-6343.
48. S. Sanz, M. Benítez and E. Peris, *Organomet.*, 2009, **29**, 275-277.
49. A. Azua, S. Sanz and E. Peris, *Chem. Eur. J.*, 2011, **17**, 3963-3967.
50. R. H. Crabtree, G. G. Hlatky, C. A. Parnell, B. E. Segmueller and R. J. Uriarte, *Inorg. Chem.*, 1984, **23**, 354-358.
51. P. Leoni, M. Sommovigo, M. Pasquali, S. Midollini, D. Braga and P. Sabatino, *Organomet.*, 1991, **10**, 1038-1044.
52. X. L. Luo, G. K. Schulte and R. H. Crabtree, *Inorg. Chem.*, 1990, **29**, 682-686.
53. M. Jang, S. B. Duckett and R. Eisenberg, *Organomet.*, 1996, **15**, 2863-2865.
54. G. E. Dobereiner, A. Nova, N. D. Schley, N. Hazari, S. J. Miller, O. Eisenstein and R. H. Crabtree, *J. Am. Chem. Soc.*, 2011, **133**, 7547-7562.
55. R. H. Crabtree, *Acc. Chem. Res.*, 1990, **23**, 95-101.
56. L. S. Lloyd, R. W. Adams, M. Bernstein, S. Coombes, S. B. Duckett, G. G. R. Green, R. J. Lewis, R. E. Mewis and C. J. Sleigh, *J. Am. Chem. Soc.*, 2012, **134**, 12904-12907.
57. R. E. Mewis, K. D. Atkinson, M. J. Cowley, S. B. Duckett, G. G. R. Green, R. A. Green, L. A. R. Highton, D. Kilgour, L. S. Lloyd, J. A. B. Lohman and D. C. Williamson, *Magn. Reson. Chem.*, 2014, **52**, 358-369.
58. G. J. Ellames, J. S. Gibson, J. M. Herbert and A. H. McNeill, *Tetrahedron*, 2001, **57**, 9487-9497.
59. C. Gaulier, A. Hospital, B. Legeret, A. F. Delmas, V. Aucagne, F. Cisnetti and A. Gautier, *Chem. Commun. (Cambridge, U. K.)*, 2012, **48**, 4005-4007.
60. H. Ibrahim, C. Gibard, C. Hesling, R. Guillot, L. Morel, A. Gautier and F. Cisnetti, *Dalton Trans.*, 2014, **43**, 6981-6989.
61. M.-L. Teyssot, A. Chevry, M. Traïkia, M. El-Ghozzi, D. Avignant and A. Gautier, *Chem. Eur. J.*, 2009, **15**, 6322-6326.
62. M.-L. Teyssot, L. Nauton, J.-L. Canet, F. Cisnetti, A. Chevry and A. Gautier, *Eur. J. Org. Chem.*, 2010, **2010**, 3507-03515.
63. A. Hospital, C. Gibard, C. Gaulier, L. Nauton, V. Thery, M. El-Ghozzi, D. Avignant, F. Cisnetti and A. Gautier, *Dalton Trans.*, 2012, **41**, 6803-6812.
64. A. J. Arduengo III, R. Krafczyk, R. Schmutzler, H. A. Craig, J. R. Goerlich, W. J. Marshall and M. Unverzagt, *Tetrahedron*, 1999, **55**, 14523-14534.
65. C. Fleckenstein, S. Roy, S. Leuthausser and H. Plenio, *Chem. Comm.*, 2007, 2870-2872.
66. S. Díez-González, in *N-Heterocyclic Carbenes* 2011.
67. C. Gibard, D. Avignant, F. Cisnetti and A. Gautier, *Organomet.*, 2012, **31**, 7902-7908.
68. T. Bernardi, S. Badel, P. Mayer, J. Groelly, P. de Frémont, B. Jacques, P. Braunstein, M.-L. Teyssot, C. Gaulier, F. Cisnetti, A. Gautier and S. Roland, *ChemMedChem*, 2014, **9**, 1140-1144.
69. M. Calligaris and O. Carugo, *Coord. Chem. Rev.*, 1996, **153**, 83-154.

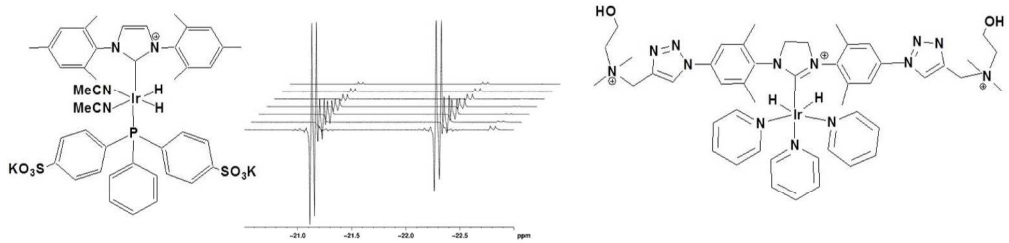

Water-soluble SABRE catalysts

209x148mm (300 x 300 DPI)